UNLIMITED

Trans 2113

(3)

ROYAL AIRCRAFT ESTABLISHMENT

Library Translation 2113

September 1983

PRACTICAL PROBLEMS WITH CO_2 LASER RADAR TESTS

by

K. Gullberg
A. Widén

Procurement Executive, Ministry of Defence
Farnborough, Hants

UNLIMITED

Translations in this series are available from:

THE R.A.E. LIBRARY
Q.4 BUILDING
R.A.E. FARNBOROUGH
HANTS

New translations are announced monthly in:

"LIST OF R.A.E. TECHNICAL REPORTS, TRANSLATIONS and BIBLIOGRAPHIES"

UNLIMITED

UDC 621.396.96 : 535.215 : 621.396.621.53 : 538.567.4 : 621.396.962.23

ROYAL AIRCRAFT ESTABLISHMENT

Library Translation 2113

Received for printing 20 September 1983

PRACTICAL PROBLEMS WITH CO_2 LASER RADAR TESTS

(ERFARENHETER FRÅN FÖRSÖK MED CO_2-LASERRADAR)

by

K. Gullberg
A. Widén

National Defence Research Institute, Stockholm, Sweden
FOA Report C 30221-E1, September 1981

Translated by
D.P. Barrett

Translation edited by
R. Hill

AUTHORS' SUMMARY

The Report describes some practical optical problems connected with beam paths and components which have arisen when operating a CO_2 laser radar at the FOA. Heterodyne detection with acousto-optical modulation and the Doppler laser radar are discussed. This work led to the laser radar which was reported under FOA Report C 30220-E1, 1981, Studies of Target Signatures with a Coherent Laser Radar by G. Bolander, K. Gullberg, I. Renhorn, O. Steinvall and A. Widén.

LIST OF CONTENTS

1 INTRODUCTION

When reporting a research project it is the practice to present the successful results and describe the apparatus which yielded the best measurements. The unsuccessful experiments carried out before that, which probably took the most time are not of interest in terms of results. On the other hand it is sometimes valuable to have these experiences documented.

This Report describes some laser radar systems which were experimented with before the one presented in FOA report C 30220-E[1]. The reasons why they were abandoned are also given. Certain frequently recurring system problems which may appear to be trivial are dealt with in detail and some common optical components are considered. The report concerns only practical optical problems.

2 LASER RADAR WITH ACOUSTO-OPTICAL MODULATION

In heterodyne detection the radiation reflected from the target is mixed with the beam from a local oscillator. If the beams are at different frequencies the difference frequency can be detected with high sensitivity, as quantum noise limited reception.

The frequency shift in this case is produced by an acousto-optical modulator as in Fig 1. The beam from the laser is divided by a beam-splitter into a transmitted beam and local oscillator beam. Mixing of the target reflection with the LO beam at the detector is done by a beam-splitter plate. The CO_2 laser is at a frequency of 28.3×10^{12} Hz (λ = 10.6 µm). The LO beam is given a frequency shift of 40 MHz, which then becomes the difference frequency which is detected. This signal is displayed on a spectrum analyser. Where there is a moving target, a Doppler shift of the frequency also occurs.

Against a target consisting of a diffusely reflecting cardboard disc at a distance of 90 m, a s/n ratio of 40 dB was obtained. This value is about 30 dB below that calculated theoretically. The principal reason for this discrepancy was an imperfection in the adjustment of the various optical components in the experimental apparatus.

2.1 The IR detector is of the CMT type, cooled by liquid nitrogen, made by Honeywell and having a high quantum efficiency. Its sensitivity was measured as 78 V/W. The optimum LO power[2] is 1 mW. Its surface measures 0.23 × 0.23 mm. The beams are focussed with a 50 mm BaF_2 lens at the detector. With a 6mm laser beam the spot diameter = $4\lambda f/\pi d \approx 0.1$ mm.

2.2 The A/O modulator, Fig 2, is of germanium, Isomet 1207A-6. It is supplied with 6 W of power at a frequency of 40 MHz and gives the same frequency shift to the LO beam together with an angular deflection. The deflection is calculated by the Bragg relation, $2\lambda_s \sin\theta = \lambda_L$, where λ_s is the acoustic wavelength, and λ_L is the wavelength of light. The velocity of sound in germanium is 5500 m/s. At 40 MHz, λ_s = 137 µm. The angle between the incoming and outgoing beams is then 2θ = 77 mrad. Our CO_2 laser has vertical polarisation, and the modulator has been aligned so that deflection occurs in the same plane.

Twelve per cent of the incident power was lost at the modulator and 20% of the transmitted power deflected onto the detector, but as a result of these losses difficulties were encountered in achieving sufficient LO power at the detector. We needed to extend the distance between the modulator and the detector lens to 200-300 mm in order to be sure of obscuring the stronger portion of the undeflected beam, otherwise there was a risk of heterodyne action between the beams, or of the detector burning out.

We never succeeded in getting rid of the powerful electrical interference at 40 MHz generated from the supply unit which entered the detector electronic circuit. In actual operation this was the main limitation on the sensitivity of our heterodyne receiver to stationary targets.

2.3 Adjustment of the beams. The signal beam and the LO beam had to be precisely adjusted to the same axis so that the wave fronts were parallel in the detector plane. Allowing 10% for heterodyne degradation, a misalignment of 10 mrad can occur, *ie* 1 mm at the beam splitter, Fig 3.

There is no great skill in drawing a diagram of an invisible weak beam path on paper. The difficulty arises in trying to get the beams to travel as devised on the diagram.

Aligning the transmitter beam and the receiver lobe and matching them to the LO beam caused us *a lot of* trouble. The following beam paths had to be adjusted.

(a) The LO beam in the modulator for maximum power in the deflected beam.

(b) Movement of the detector and lens in the X, Y and Z axes to get the maximum LO signal at the detector.

(c) Matching of the transmitted laser beam with the receiver lobe.

(d) Alignment and focussing the receiver optical system so that the detector gave the maximum signal.

(e) Matching the beam paths from the receiver optical system with the LO beam.

A HeNe laser was used as an aid to initial alignment and chopping techniques for final optimisation. It was only during the final alignment that we were able to obtain a heterodyne signal on which to optimise.

The experiments with the acousto-optical laser radar were discontinued because of the difficulties described above with the 40 MHz electrical interference, the adjustment of the beams and the fact that adequate LO power was never obtained.

3 DOPPLER LASER RADAR

We have tested another system with which we can detect only moving targets by means of Doppler shift of the laser frequency, Fig 4.

As in the previous system, the laser beam is divided into a transmitter beam and a LO beam. The received beam is mixed with the LO beam at the detector, which produces a Doppler shift from the moving target, $\Delta f = 2v/\lambda$, where v is the speed of the target. If v is 1 m/s then $\Delta f = 200$ kHz.

For the adjustment of the Doppler system a rotating arm with two paddles covered with aluminium-coated emery cloth was used which had a peripheral velocity of 1 m/s.

This system was used to monitor motor vehicles passing along a road 2 km away, Fig 5. The signal was displayed on a spectrum analyser without any processing.

During initial tests it was found that the receiver optical system was not correctly adjusted. The reflected beam was being incorrectly intercepted by the transmitter reflector and was being reflected back to the laser to follow the same path as the LO beam.

It was realised that it is not easy to manage two separate optical systems for the transmitter and the receiver, which have to be aligned on the same axis, focussed at the same distance, and matched to the LO beam.

Instead, we then tried a *Michelson interferometer type of Doppler system*, with one telescope instead of two telescopes. The advantage of a common optical system for transmission and reception is that the incoming and outgoing beams follow the same path, and focussing is therefore common. The principle is illustrated in Fig 6. The beam from the laser is divided by a beam splitter set at an angle of 45° to the incident beam. The LO beam is reflected back to the detector, where it is mixed with the return from the target. The beams are focussed on to the detector by a lens.

One difficulty with this system is to get the optimum LO power at the detector. The optimum is 1 mW, and too high a power saturates the detector. Also multiple reflections from a plane-parallel beam splitter lie too close together for us to be able to screen them out (1 mm with a 4mm plate). This problem was solved in the following way.

3.1 Wedge-shaped beam-splitter

In both of the Doppler arrangements we used a wedge-shaped beam splitter of germanium and selected a suitable multiple reflection for the LO beam. The plate had a wedge angle of 0.76°. The disadvantage, of course, is that this produces attenuation in relatively large discrete steps, which seriously limits its use. In the first Doppler arrangement, Fig 4, we were lucky enough to get the LO power at the detector just right, though with the Michelson system we were forced to use a mirror of low reflectance in order to attenuate further the beam. Fig 6 illustrates how the wedge plate operated in the Michelson system. The numbers indicate the strengths of the transmitter, receiver and LO beams.

With this arrangement we lost three-quarters of the transmitted laser power I_0 through the wedge plate. The received signal I_s is also attenuated by half when reflected to the detector.

This solution afforded us a more easily manageable optical system for transmitter and receiver alignment but the problem of optimising the LO beam remained. Another disadvantage was losses in the beam splitter. A proposal for a better solution is illustrated in Fig 7. In this configuration the wedge-shaped germanium beam splitter plate was placed at the Brewster angle, so that the transmitted beam, which had a polarisation parallel to the plane of incidence, passed through it unobstructed apart from a minor portion which was used for the LO beam. For effective reflection of the return signal from the target

to the detector to be achieved by the beam splitter the plane of polarisation had to be rotated through 90^{o}. This was achieved in two stages using a $\lambda/4$ plate. The LO beam was the first multiple reflection from the beamsplitter which was reflected back to the detector. The plane of polarisation had also to be rotated by a $\lambda/4$ plate to obtain the same polarisation as that of the signal beam.

With this arrangement 94% of the laser power should be emitted, and 66% of the signal from the target should reach the detector. The corresponding figures for the system shown in Fig 6 are five times worse, 25% and 48%.

4 THE LASER

A 5W vertically polarised Sylvania 948 CO_2 laser was used. It had a guaranteed service life of 1 year and was purchased in 1971. When the gas has degenerated it ceases to function and it may then be returned to the USA for replenishment of the gas at a cost of circa £400. It was decided instead to break the glass seal and fit it with a Nupro metal valve. Using a vacuum system a glass container was filled with a suitable mixture of gas:

H_2	0.5%
Xe	5%
N_2	13.5%
CO_2	24%
He	57%

From this storage vessel the laser could be replenished as required to a pressure of 14 torr (1.9 kPa).

The laser was not at all stable, it drifted in frequency and the laser line changed with variations in temperature. Using a thermostatically-controlled closed-circuit cooling system the drift was substantially reduced and a suitable laser line was selected by means of piezo-electric control. However it continued to drift somewhat, and sometimes the beam changed from the single mode to some higher mode, which caused the circular Gaussian-distributed beam to change into something resembling a coffee bean. The laser beam had to be monitored occasionally during operation.

4.1 Indicators for the CO_2 laser beam

Powers down to a few watts are easily indicated by a small asbestos disc which becomes incandescent on the surface. Weaker beams produce black marks on Thermofax paper. Still weaker beams are indicated by a leaf of liquid crystal (Edmon Sci. Co) or by a UV-irradiated phosphor screen.

Asbestos and paper are continually evaporating organic substances away, which tend to cause deposits on the optical components if one gets too close. This easily contaminates them, and it is therefore difficult to know for certain where the beam is striking the reflector or some other component. It is often possible to use a HeNe laser to align optical components.

4.2 Attenuation of the CO_2 laser beam

can be performed by several means all of which have their limitations. In the literature there are all kinds of sophisticated attenuators to be found, which as a rule are too complicated to be of interest in this connection.

(a) Beam power can be continuously reduced with a variable diaphragm. Some unexpected trouble however can be caused by diffraction effects.

(b) Absorbent filters may become warm, and vary their properties. We have not found any good neutral density filters which have constant attenuation over the spectral range of the CO_2 laser from 9.4 to 10.5 μm. Potential materials generally have their absorption edge in the range itself. For example a 10mm CaF_2 plate has 5% transmission at 10.6 μm and 30% at 9.4 μm. Should the laser happen to shift its wavelength which occurs now and again, it may have serious consequences.

(c) If the laser is polarised it is possible to produce attenuation with two Brewster windows which can be rotated in the beam axis. The drawback is that the plane of polarisation of the attenuated beam is also rotated.

(d) If the beam is weak, attenuation can be achieved using plastic foil[3].

5 REFLECTIONS FROM THE TELESCOPE

A reflecting telescope which is used simultaneously for transmission and reception, Fig 8, may give an extra dose of local oscillator power because some of the transmitted beam is reflected back by the small secondary reflector through the hole in the primary mirror and is collected by the lens on the detector. However this reflection is not focussed in the plane of the detector but a little behind it. When the lens in our system was stopped down this reflection was not noticed. A telescope system having a lens which is superior in this respect is shown in Fig 9. A diaphragm can be placed in the focal plane, thereby limiting the solid angle of the reflection by the secondary mirror. However an additional optical component has been introduced which complicates the alignment. The lens should, of course, be anti-reflection coated so as to reduce surface reflections. A meniscus lens is to be preferred as it enables one to obtain a greater angle of curvature. Still more effective is an 'off axis' system, Fig 10, where no reflection is returned at all.

6 BEAM-SPLITTER PLATES

When using beam-splitter plates the reflectance and transmittance characteristics need to be known. These are dependent on the index of refraction of the material, the angle of incidence and the polarisation of the beam. The reflectance characteristic is calculated from the refraction formula $n_1 \sin\alpha = n_2 \sin\beta$ and Fresnel's formulae.

$$R_{\perp} = \left(\frac{\sin(\alpha - \beta)}{\sin(\alpha + \beta)}\right)^2 \qquad \text{for a beam polarised perpendicularly to the plane of incidence} \qquad (1)$$

$$R_{//} = \left(\frac{\tan(\alpha - \beta)}{\tan(\alpha + \beta)}\right)^2 \qquad \text{for a beam polarised parallel to the plane of incidence} \qquad (2)$$

Transmittance is calculated by the same formulae assuming that both faces of the plate reflect equally and is $(1 - R_1)^2$, where R_1 is either $R_{\perp}$ or $R_{//}$.

On several occasions it was necessary to allow for the parallel-shifted multiple reflections which occurred in the plate. Though these are weaker than the primary reflections they may sometimes cause complications. In some cases they can actually be useful, *eg* if it is desired to attenuate the beam. The obscuration of multiple reflections is more difficult for thin plates.

The paths of the beams through a beam-splitter plate and the formulae for the calculation of their strengths are illustrated in Fig 11. R_1 is calculated by either of Fresnel's formulae (1) and (2).

Fig 12 shows this parallel shifting process and the calculation of the distance between multiple beams.

Tables 1 and 2 contain the calculated reflectance and transmittance values for the first three beams in three common IR materials for a beam-splitter having a 45° angle of incidence.

In Table 3, the distance between multiple beams, due to this parallel shifting process, is calculated for two different thicknesses of beam-splitter plate. It can be seen that for materials with a high refractive index the interval between the exit points of the beams along the plate will be large, but due to the value of the exit angle the perpendicular distances between the beams will be small.

7 FOCAL LENGTH OF LENSES FOR IR

The focal length of a lens varies considerably between that in the visible and the 10 μm regions owing to dispersion.

When a lens is focussed by means of a HeNe laser it does not always agree with that obtained using a CO_2 laser. When selecting a lens one should consider the wavelength to which the stated focal length applies.

Focal length can be expressed as

$$\frac{1}{f} = \left(\frac{n_2}{n_1} - 1\right)\left(\frac{1}{r_1} + \frac{1}{r_2}\right) \qquad (3)$$

where n_1 is the refractive index of the ambient medium, n_2 is the index of refraction of the lens, and r_1 and r_2 the radii of curvature of the lens.

When a wavelength is varied from $\lambda 1$ to $\lambda 2$, the focal length is then varied for the same lens in air according to the relationship:-

$$f_{\lambda 2} = f_{\lambda 1} \frac{n_{\lambda 1} - 1}{n_{\lambda 2} - 1} \qquad (4)$$

Table 4 gives some examples of the difference in focal length for the visible and the 10 μm region.

Table 1

BEAM-SPLITTER PLATES
(Reflectance and transmittance for beams polarised perpendicularly to the plane of incidence and at an angle of incidence of 45°)

Material	n_λ = 10 μm	Angle of incidence	R_1	R_2	R_3	T_1	T_2	T_3
Ge	4.0	45°	0.484	0.129	0.030	0.267	0.062	0.015
ZnSe	2.408	45°	0.281	0.145	0.011	0.517	0.041	0.003
NaCl	1.50	45°	0.0920	0.0759	0.0006	0.824	0.0070	0.00006

Table 2

BEAM-SPLITTER PLATES
(As above, with polarisation parallel to plane of incidence)

Material	n_λ = 10 μm	Angle of incidence	R_1	R_2	R_3	T_1	T_2	T_3
Ge	4.0	45°	0.234	0.137	0.0075	0.587	0.0321	0.0018
ZnSe	2.408	45°	0.0789	0.0669	0.00042	0.848	0.0053	3×10^{-5}
NaCl	1.50	45°	0.0085	0.0083	6×10^{-7}	0.983	7×10^{-5}	5×10^{-9}

Table 3

BEAM-SPLITTER PLATES
(Parallel shift of a through beam and distance between multiple reflections for plates of two thicknesses)

Material	Angle of incidence	Parallel shift of through beam		Distance between multiple reflections	
		t = 1 mm	t = 4 mm	t = 1 mm	t = 4 mm
Ge	45°	0.58 mm	2.32 mm	0.25 mm	1.02 mm
ZnSe	45°	0.49 mm	1.96 mm	0.43 mm	1.74 mm
NaCl	45°	0.33 mm	1.32 mm	0.76 mm	3.02 mm

Table 4

TABLE OF REFRACTIVE INDICES FOR SOME IR MATERIALS AND EXAMPLES OF FOCAL LENGTHS IN THE CO_2 LASER RANGE FOR LENSES HAVING f = 100 mm IN THE VISIBLE RANGE

Material	Wavelength (μm)	n	Focal length (mm)
ZnSe	0.656	2.578	100
	10	2.408	112
BaF_2	0.6	1.458	100
	10.34	1.396	116
CaF_2	0.6	1.426	100
	9.724	1.308	138
NaCl	0.640	1.541	100
	10.02	1.495	109

REFERENCES

No.	Author	Title, etc
1	G. Bolander K. Gullberg I. Renhorn O. Steinvall A. Widén	Studies of target signatures with a coherent laser radar. FOA report C 30220-E1 (1981)
2	S. Lundqvist H. Eklund	Noise measurements in a HgCdTe photodiode. Chalmers Tekniscka Högskola Technical Report 7861 (1978)
3	K. Gullberg O. Strömberg	Transmission curves in the IR range for plastics. FOA report C 30090-E8 (1976)

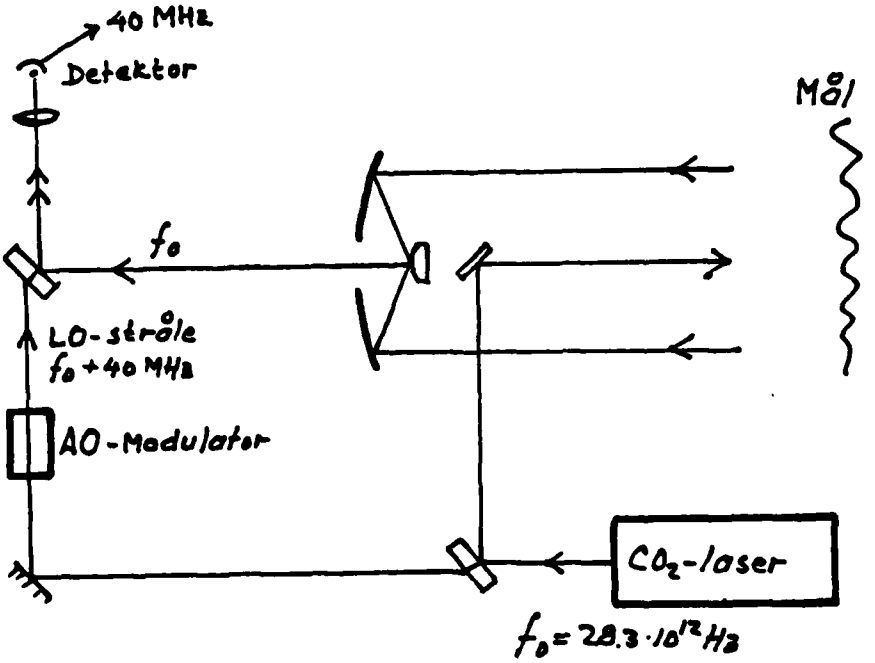

Key:
LO-stråle = local oscillator beam f_0 + 40 MHz
Mål = target

Fig 1 Laser radar with acousto-optical modulation

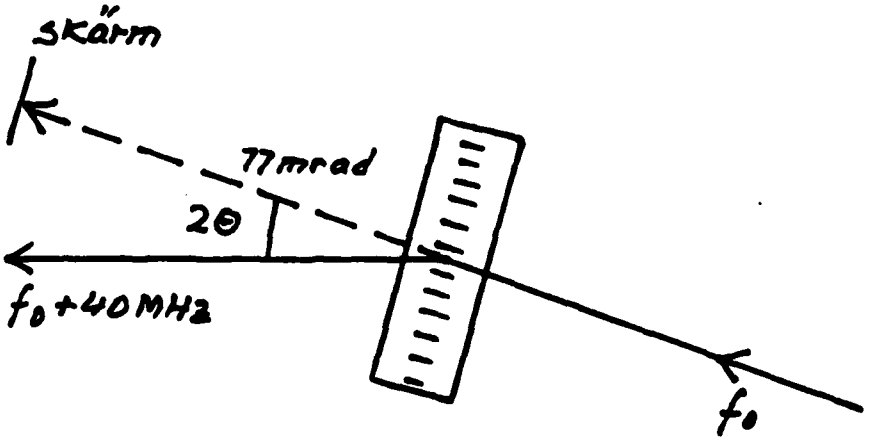

Key:
Skärm = screen

Fig 2 Acousto-optical modulator

Fig 3

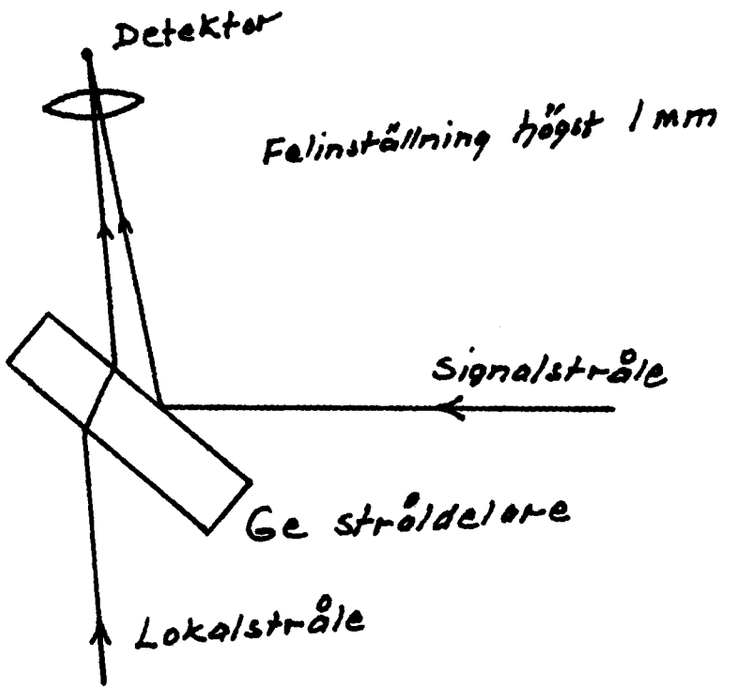

Key:
Felinställning högst = maladjustment maximum 1 mm
Signalstråle = signal beam
Ge stråldelare = Ge beam-splitter
Lokalstråle = local oscillator beam

Fig 3 Maladjustment of a beam-splitter

LT 2113

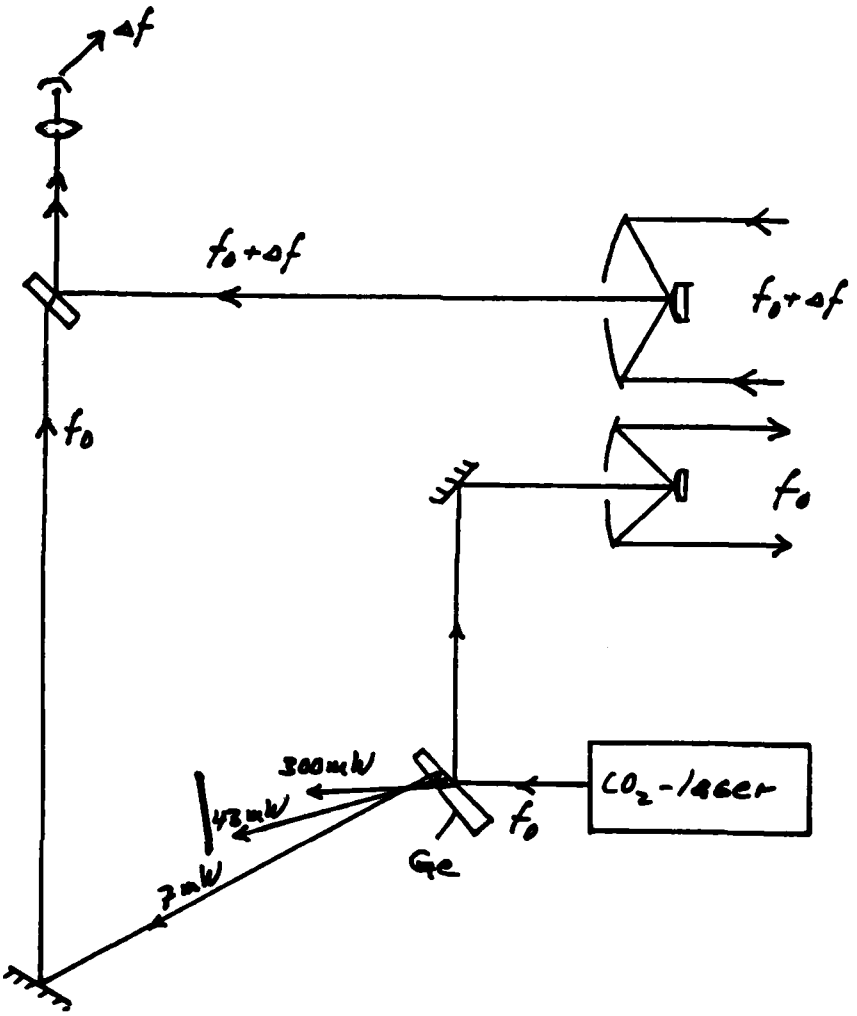

Fig 4 Doppler laser radar

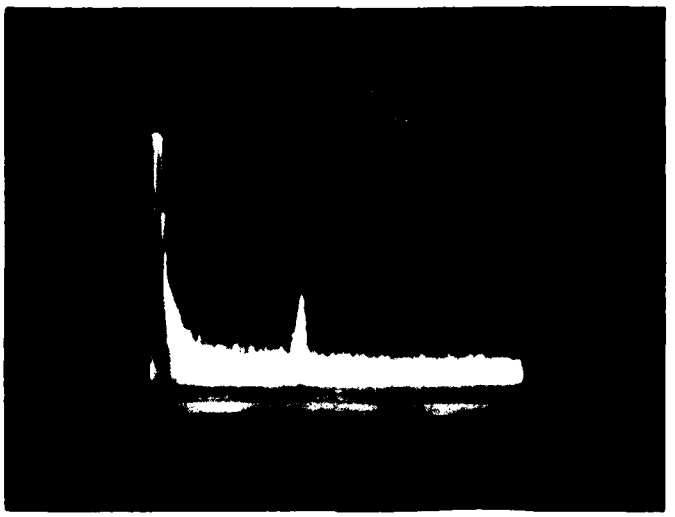

Fig 5 Monitoring of a vehicle 2 km away with the Doppler laser radar (100 kHz/div, height scale 20 dB/div)

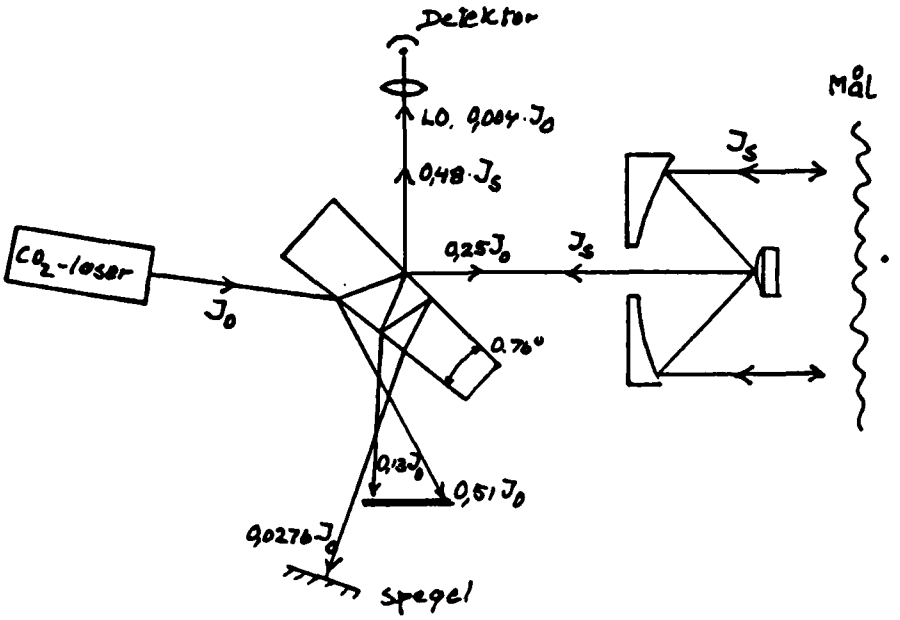

Fig 6 Doppler system using a Michelson interferometer. Beam path and attenuation of reflections in the beam-splitter plate

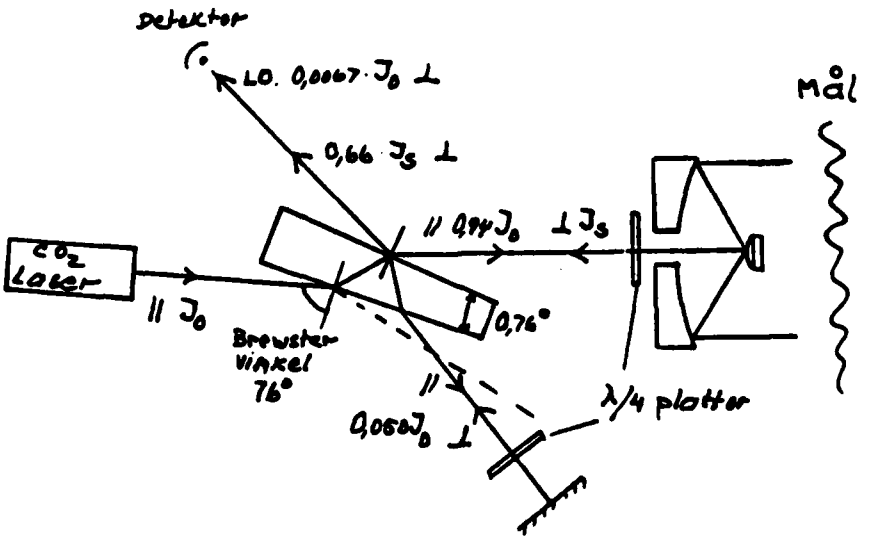

Fig 7 Sketch of Michelson interferometer Doppler system. The germanium beam-splitter is placed at the Brewster angle, giving high efficiency

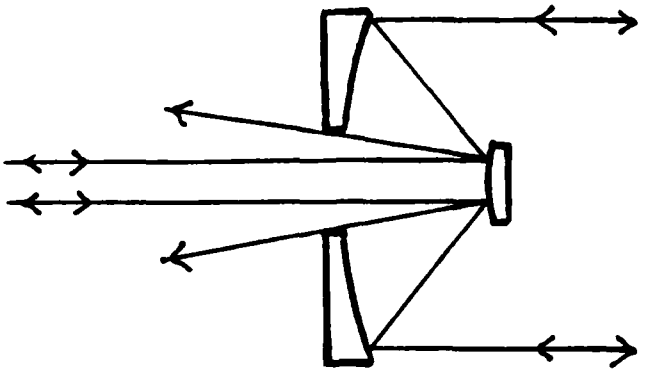

Fig 8

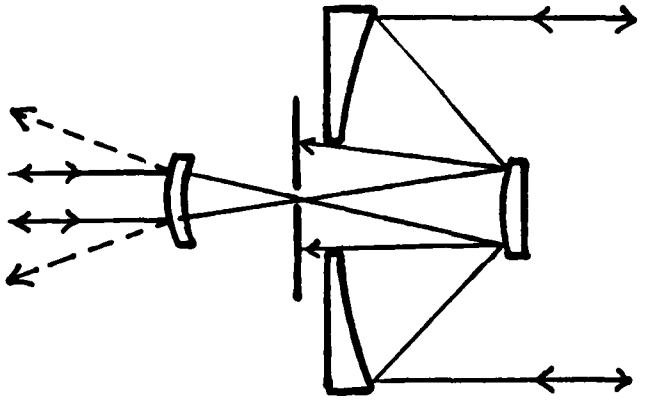

Fig 9

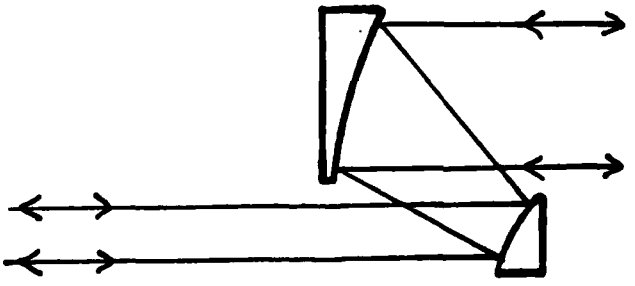

Fig 10

Figs 8-10 Back reflections by a telescope when used for both transmission and reception

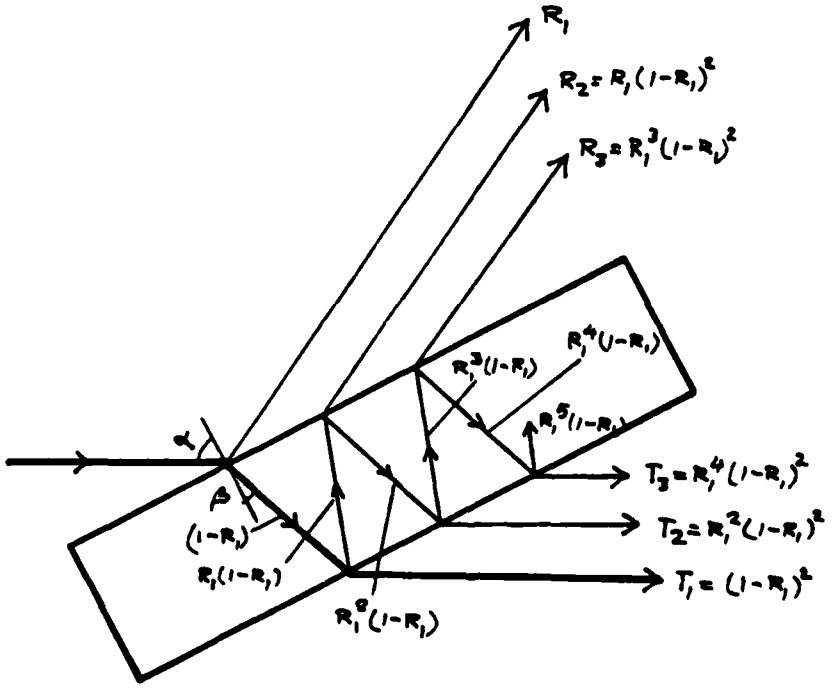

Fig 11 Reflectance and transmittance with multiple reflections in a beam-splitter plate

Parallellförskjutning b
av stråle i stråldelare

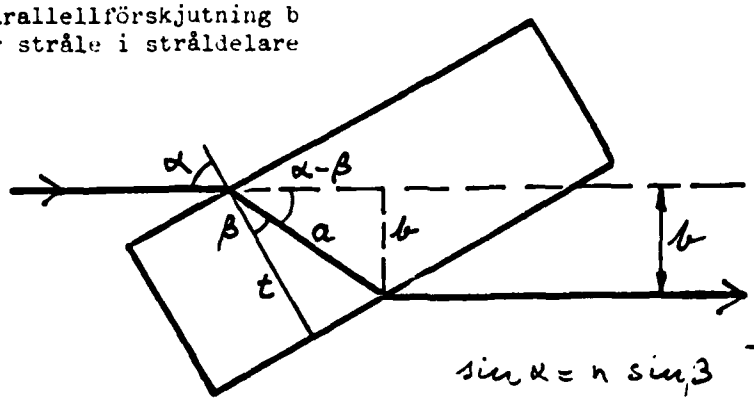

$$\sin\alpha = n \sin\beta$$
$$a = \frac{t}{\cos\beta}$$
$$b = a \sin(\alpha-\beta)$$
$$b = \pm \frac{\sin(\alpha-\beta)}{\cos\beta}$$

Avstånd mellan multipla reflexer

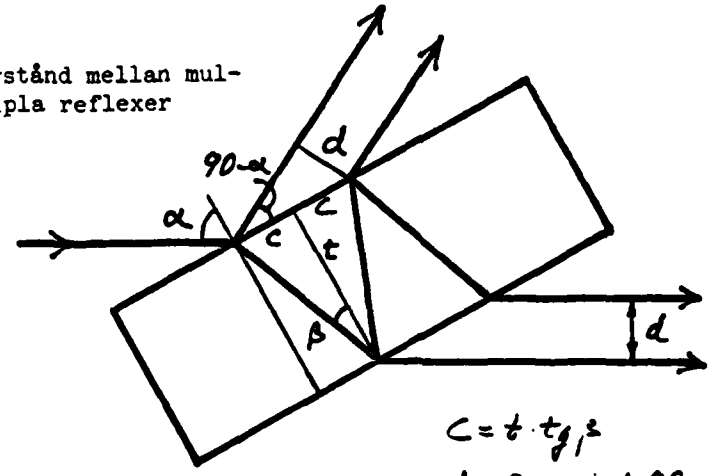

$$c = t \cdot tg\beta$$
$$d = 2c \sin(90-\alpha)$$
$$d = 2t \cdot tg\beta \cdot \sin(90-\alpha)$$

Key:
Parallellförskjutning b av stråle i stråldelare = parallel shifting b of a beam in the beam-splitter
Avstånd mellan multipla reflexer = distance between multiple reflections

Fig 12 Parallel shifting and distance between multiple reflections in a beam-splitter plate